Contents lists available at ScienceDirect

Arabian Journal of Chemistry

journal homepage: www.ksu.edu.sa

Original article

Heavy metal(loid)s contamination and ecological-health risk assessment of coastal sediment from Salwa Bay, Saudi Arabia

Khaled Al-Kahtany, Mansour H. Al-Hashim, Abdelbaset S. El-Sorogy *

Geology and Geophysics Department, College of Science, King Saud University, P. O. Box 2455, Riyadh 11451, Saudi Arabia

ARTICLE INFO

Keywords:
Arsenic
Chromium
Lead
Zink
Cupper
Coastal sediment

ABSTRACT

Salwa Bay is an elongated, narrow bay which extends southwards from the Gulf of Bahrain down to the Saudi-Qatari border, separating the peninsula of Qatar from Saudi Arabia. The present study aims to investigate the degree of heavy metal(loid)s (HMs) contamination and the associated health risks in surface sediments of the Salwa Bay, Saudi Arabia. Thirty samples were collected for analysis of Ni, Cu, Cr, Pb, Zn, and As using inductively coupled plasma-atomic emission spectrometry (ICP-AES). Several contamination and health risk indices, and multivariate analysis were applied. The following order was detected for average concentrations of metal (loid)s (μg/g dry weight): Cr (5.56) > Zn (4.63) > Ni (4.43) > As (2.34) > Pb (1.66) > Cu (1.51). The coastal sediments exhibit a significant enrichment in As, moderate enrichment in Pb, Zn, Cr, and deficiency to minimal enrichment for Ni, and Cu. Sediment quality guidelines indicated that HMs do not pose a risk to the benthic communities in Salwa Bay area. The average hazard index values ranged from 0.00002 to 0.0038 in adults and from 0.0002 to 0.0353 in children. This suggests that there is no significant possibility of non-carcinogenic effects to the people inhabiting the coastline of Salwa Bay. The results of the excess lifetime cancer risk (ELCR) for As, Cr, and Pb were below 1×10^{-4}, indicating no carcinogenic health risk except for a few sediment samples showing elevated levels of Cr and As.

1. Introduction

Rising human populations lead to an escalation in air, land, and water pollution. The breakdown of mafic and ultramafic rocks results in the release of heavy metal(loid)s (HMs) like copper, lead, zinc, chromium, nickel, and cadmium into the soil and nearby water bodies (Al-Kahtany and El-Sorogy, 2022, 2023). Principal anthropogenic sources contributing to HM pollution in coastal sediment include wastewater irrigation, metal-based pesticides or herbicides, phosphate-based fertilizers, sewage effluents, and petroleum distillate spillage (Al-Hashim et al., 2021; Alzahrani et al., 2023a; El-Sorogy et al., 2023).

HMs are of significant concern due to their detrimental impact on ecosystems and human health. Elevated levels of HMs can harm aquatic ecosystems and their associated biota, leading to structural modifications in aquatic life, particularly fish, resulting in a decline in their populations. HMs exceeding permissible limits profoundly alter water quality, acting as toxins which may accumulate extensively in the tissues of aquatic organisms, particularly fish, negatively affecting the quality and quantity of fish populations (Shah et al., 2012; Luo et al., 2014; Mohammadi et al., 2022; Alzahrani et al., 2023b).

The release of HMs into aquatic environments leads to their accumulation in marine sediments, presenting an ecological hazard to filter-feeder organisms and ultimately impacting humans (El-Sorogy and Youssef, 2015; Singovszka et al., 2017; Demircan et al., 2023). Despite the essential nature of certain HMs such as manganese, iron, copper, nickel, lead, and zinc, which are all required in minimal quantities and are recognized as nutritionally essential, excessive exposure to these HMs can be toxic and may result in severe health issues including cancer, diabetes, asthma, respiratory distress, cardiovascular diseases, and neurodegenerative disorders (Abbaspour et al., 2014; Alharbi and El-Sorogy, 2023). Children, being particularly sensitive to heavy metal (loid)s, experience additional exposure routes through breastfeeding, placental exposure, hand-to-mouth activities during early years, and lower toxin elimination rates (Ma et al., 2016; Rahman et al., 2021; Kahal et al., 2023). Furthermore, chronic arsenic ingestion may lead to lung diseases like chronic bronchitis, chronic obstructive pulmonary disease, and bronchiectasis, as well as liver problems such as non-cirrhotic portal fibrosis (Mazumder, 2008; Alharbi et al., 2023).

* Corresponding author.
E-mail address: asmohamed@ksu.edu.sa (A.S. El-Sorogy).

https://doi.org/10.1016/j.arabjc.2024.105868
Received 14 March 2024; Accepted 9 June 2024
Available online 15 June 2024

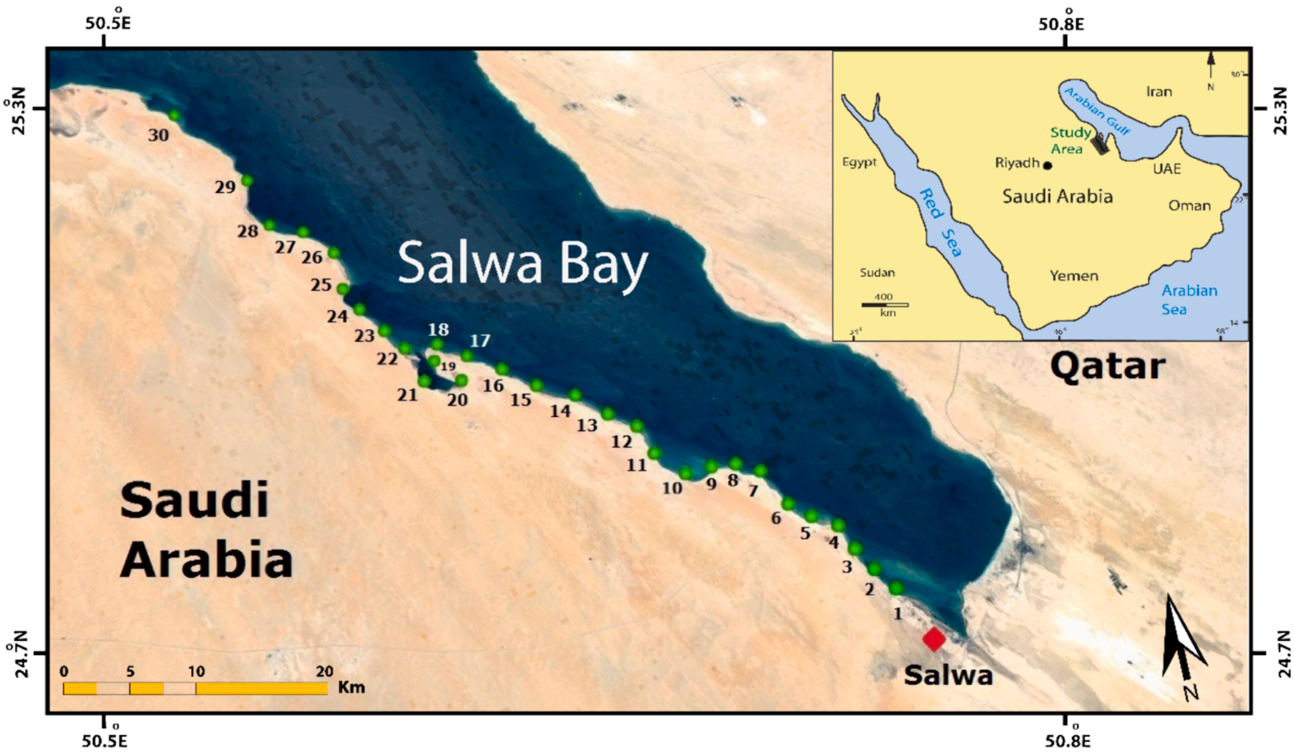

Fig. 1. Location map of the sampling sites along Salwa Bay.

During the last two decades, extensive environmental research has indicated a swift decline in the coastal ecosystems of the Arabian Gulf, primarily due to human activities (e.g., de Mora et al., 2004; Naser, 2013; Almahasheer et al., 2013; Almasoud et al., 2015; El-Sorogy et al., 2019, 2024). In a recent study focusing on the distribution of seashells in Salwa Bay, El-Sorogy et al. (2024) identified 48 species of rocky shore epi-faunal and shallow sandy bottom in-faunal invertebrates. The Veneridae, Trochidae, and Acroporidae were reported to be the most abundant bivalve, gastropod, and coral families, respectively. However, there has been no study examining human health in Salwa Bay, specifically using risk indices to evaluate the hazard and excess lifetime cancer risk (ELCR) associated with ingestion and dermal contact for both adults and children. Consequently, the current research aims to: (i) determine the levels and document the distribution of As, Ni, Zn, Cr, Pb, and Cu in marine sediments along Salwa Bay, Saudi Arabia; (ii) assess the degree of contamination by these HMs using enrichment factor, geo-accumulation index, and contamination factor; and (iii) establish the carcinogenic and possibility of non-carcinogenic effects posed by these substances using hazard index and excess lifetime cancer risk.

2. Material and methods

2.1. Study area

Salwa Bay represents the most saline extension of the Arabian Gulf. It is situated as a landlocked cul-de-sac between Saudi Arabia and Qatar (Fig. 1). The hypersalinity is attributed to coral-reef barriers at the bay's entrance, the shallow nature of the basin (water depths are less than 10 m), and the slow flushing rates leading to prolonged residence times of the waters (Basson et al., 1977; Amao et al., 2018, El-Sorogy et al., 2024). Seashells and coral fragments along the Bay coastline undergo bio-erosion by various mollusks and annelids, similar to observations in other locations along the Red Sea and Arabian Gulf coastlines (El-Sorogy, 2015; El-Sorogy et al., 2018, 2020, 2021; Demircan et al., 2021, 2023; El-Sorogy and Alzahrani, 2024). Floral and faunal diversities have been noted to decline towards the bay interior, mirroring the salinity gradient (Clarke and Keij, 1973; Riera et al., 2011).

2.2. Sampling and analytical methods

Thirty sediment samples were taken from the Salwa Bay coastal zone (Fig. 1), stored in plastic bags, and kept in an icebox. In the lab, the samples were air-dried at temperatures ranging from 18 to 26 °C for a week, following the removal of sea grass and gravels. Subsequently, the samples underwent size fractionation using a set of sieves to isolate the < 63 µm fraction for analysis. A prepared sample (0.50 g) was digested with HNO_3-HCl aqua regia for 45 min in a graphite heating block. The resulting solution was then diluted to 12.5 mL with deionized water, mixed, and subjected to analysis. Cr, Cu, As, Ni, Pb, and Zn were analyzed using inductively coupled plasma-atomic emission spectrometry (ICP-AES) at the ALS Geochemistry Lab in the Jeddah branch, Saudi Arabia. The ICP-AES method underwent validation for linearity, limits of detection (LOD), limits of quantification (LOQ), accuracy, and precision. Calibration curves were established for each element by plotting the peak area of the optimum emission line against the concentration of standard solutions or spike solutions for standard addition curves. The calibration curves demonstrated excellent linearity for all elements. The relative standard deviations (RSD%) for all metal(loids) were below 13.5 %, indicating the method exhibited satisfactory precision, as reported by Manousi and Zachariadis in 2020. The relative recovery values (R%) fell within the range of 80–120 %, affirming the method's accuracy.

HMs contamination in sediment samples was evaluated using the enrichment factor (EF), geoaccumulation index (Igeo), and contamination factor (CF) as outlined by Kowalska et al. (2018). The formulas for these indices are derived from the works of Hakanson (1980), El-Sorogy and Attiah (2015), Weissmannová and Pavlovský (2017):

$$EF = \left(\frac{M}{X}\right)_{sample} / \left(\frac{M}{X}\right)_{background} \tag{1}$$

Table 1
Exposure factors used in estimation of chronic daily intake (CDI) for non-carcinogenic.

Parameter	Units	Adults	Children
Ingestion rate (IngR)	mg/day	100	200
Exposure frequency (EF)	days/year	350	350
Exposure duration (ED)	year	24	6
Body weight (BW)	Kg	70	15
Average Time for possibility of non-carcinogenic effects (AT_{nc})	days	8760	2190
Average Time for carcinogenic risk (AT_c)	days	25,550	25,550
Skin surface area (SA)	cm^2	5700	2800
Adherence factor (AF)	mg/cm	0.07	0.2
Dermal absorption factor (ABS)	–	0.001	0.001
Conversion factor (CF)	Kg/mg	10^{-6}	10^{-6}
Concentration of heavy metal(loid)s (C)	Mg/kg	–	–

Table 2
The reference dose (RfD) and the cancer slope factors (CSF) for HMs.

HMs	RfDing	RfDderm
Cr	3×10^{-3}	6×10^{-5}
Cu	4×10^{-2}	4.02×10^{-2}
Ni	2×10^{-2}	5.4×10^{-3}
Zn	3×10^{-1}	6×10^{-2}
Pb	3.5×10^{-3}	3.25×10^{-4}
As	3×10^{-4}	1.23×10^{-4}
HMs	**CSFing**	**CSFderm**
As	1.5	3.66
Pb	0.0085	–
Cr	0.5	20

$$I_{geo} = Log_2\left(\frac{C_n}{(1.5 \times B_n)}\right) \quad (2)$$

$$CF = C_o/C_b \quad (3)$$

M and Co represent the concentrations of the analyzed metal, while X and Cb signify the levels of a normalizer element. Iron (Fe) is frequently employed as a normalizing element in this study due to its high abundance in the Earth's crust and its limited movement in most natural settings compared to other trace elements. As a result, it serves as a reliable reference point for evaluating the natural background levels of other elements (Alzahrani et al., 2023a). Cn is the measured concentration of the HMs in the soils, Bn is the geochemical background concentration of the HMs in shale, and 1.5 is introduced to minimize the effects of possible variations in the background values.

To estimate health risks associated with ingestion and dermal contact pathways for both adults and children, various indices such as chronic daily intake (CDI), hazard quotients (HQ), hazard index (HI), cancer risk (CR), and excess lifetime cancer risk (ELCR) can be computed. The formulas for these indices are derived from the works of Luo et al. (2012), IRIS (2020), and Miletic et al. (2023).

$$CDI_{ing} = \frac{(C_{sediment} \times IngR \times EF \times ED)}{(BW \times AT)} \times CF \quad (4)$$

$$CDI_{derm} = \frac{(C_{sediment} \times SA \times EF \times ED)}{(BW \times AT)} \times CF \quad (5)$$

$$HQ = CDI/RfD \quad (6)$$

$$HI = \sum HQ = HQ_{ing} + HQ_{derm} \quad (7)$$

$$CancerRisk = CDI \times CSF \quad (8)$$

$$ELCR = \sum CancerRisk = CancerRisk_{ing} + CancerRisk_{derm} \quad (9)$$

Table 1 illustrates the exposure factors which were utilized in estimating chronic daily intake (CDI) for possibility of non-carcinogenic effects (USEPA, 2002; Chen et al., 2022; Miletic et al., 2023). The Environmental Protection Agency (EPA) supplies reference dose (RfD) values for all examined HMs for ingestion exclusively (USEPA, 2023). The impact of Pb on humans via dermal contact is uncertain; hence, CSF values for dermal contact with Pb were scarcely referenced in Table 2 (Miletic et al., 2023).

3. Results and discussion

3.1. Concentration and distribution of heavy metal(loid)s

The concentrations of HMs, presented in Table S. 1 in μg/g (dry weight), followed a descending order as Cr (5.56), Zn (4.63), Ni (4.43), As (2.34), Pb (1.66), and Cu (1.51). Fig. 2 presents the distribution of metal(loid)s per studied sites. the highest concentrations of metal(loid)s were observed in sample 1 (Cr, Cu, and Pb), sample 9 (As), and sample

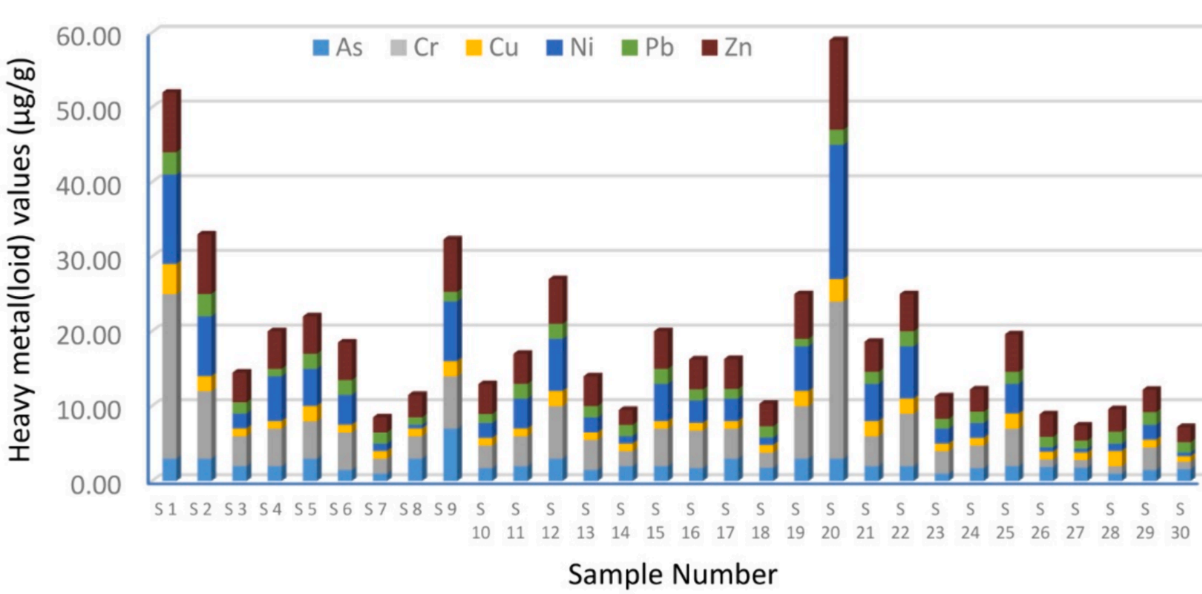

Fig. 2. Distribution of heavy metal(loid)s in sediments obtained from Salwa Bay area.

Table 3
Comparison between the average HM values (μg/g) in Salwa bay and worldwide background references and SQGs.

Location and references		As	Zn	Ni	Cr	Pb	Cu
Salwa Bay, Saudi Arabia (present study)		2.34	4.63	4.43	5.56	1.66	1.51
Southeastern Black Sea (Aydin et al., 2023)		13.66	155.03	44.93	120.75	93.71	82.66
Ras Abu Ali, Arabian Gulf (Al-Kahtany and El-Sorogy, 2023)		2.47	6.89	13.00	7.86	3.50	4.14
Giresun, southeast Black Sea (Kodat and Tepe, 2023)		7.36	94.16	27.29	60.64	41.37	45.66
Aqeer coastline, Arabian Gulf (Al-Hashim et al., 2021)		14.99	7.62	0.57	3.67	3.88	11.27
Yanbu coastline, Saudi Arabia (El-Sorogy et al., 2021)		6.83	80.4	23.5	27.11	7.72	35.87
Red Sea-Gulf of Aqaba coastline (El-Sorogy et al., 2020)		133	24.0	14.0	39.0	6.60	30.0
Al-Khobar, Saudi Arabia (Alharbi and El-Sorogy, 2017)		1.61	52.7	75.0	51.03	5.36	183
Al-Jubail – Al-Khafji, Arabian Gulf (Alzahrani et al., 2023)		2.38	6.18	11.76	8.68	2.57	2.44
Background shale (Turekian and Wedepohl, 1961)		13	95	68	90	20	45
Background continental crust (Taylor, 1964)		1.8	70	75	100	12.5	55
Sediment quality guidelines	Effects range-low (ERL)	8.2	150	20.9	81	46.7	34
(Long et al., 1995)	Effects range-median (ERM)	70	410	51.6	370	218	270

Table 4
Class distribution (sample %) of geo-accumulation index, enrichment factor, and contamination factor for HMs examined in the sediment samples of the study area.

Indices	Classes			As	Cr	Cu	Ni	Pb	Zn
	Class 1	EF < 2	Deficiency to minimal enrichment	0	70	80	60	13.33	70
	Class 2	EF = 2–5	Moderate enrichment	26.67	30	16.67	40	60	30
	Class 3	EF = 5–20	Significant enrichment	66.67	0	3.33	0	26.67	0
EF	Class 4	EF = 20–40	Very high enrichment	6.66	0	0	0	0	0
	Class 5	EF > 40	Extremely high enrichment	0	0	0	0	0	0
	Class 1	Cf < 1	Low contamination factor	100	100	100	100	100	100
CF	Class 2	1 ≤ Cf < 3	Moderate contamination factor	0	0	0	0	0	0
	Class 3	3 ≤ Cf < 6	Considerable contamination factor	0	0	0	0	0	0
	Class 4	Cf ≥ 6	Very high contamination factor	0	0	0	0	0	0
	Class 0	Igeo < 0	uncontaminated	100	100	100	100	100	100
	Class 1	0 < Igeo < 1	unpolluted to moderately contaminated	0	0	0	0	0	0
	Class 2	1 < Igeo < 2	moderately contaminated	0	0	0	0	0	0
Igeo	Class 3	2 < Igeo < 3	moderately to strongly contaminated	0	0	0	0	0	0
	Class 4	3 < Igeo > 4	Strongly contaminated	0	0	0	0	0	0
	Class 5	4 < Igeo < 5	Strongly to extremely contaminated	0	0	0	0	0	0
	Class 6	Igeo > 5	Extremely high contaminated	0	0	0	0	0	0

20 (Ni and Zn). Conversely, the lowest values for heavy metals were reported in samples located in the central to northern part of the bay (e.g., samples 19, 21, 23, and 26–30).

The background values were taken as a reference for later studies from a long time ago, because a new determination was not made considering areas of anthropic effect. The average concentrations of Cu, Ni, Pb, and Zn in Salwa Bay, as presented in Table 3, were found to be lower than those reported from various coastal areas, including the Arabian Gulf, background references, and the south-eastern Black Sea (Al-Hashim et al., 2021; Al-Kahtany and El-Sorogy, 2023; Alharbi and El-Sorogy, 2017; Turekian and Wedepohl, 1961; Taylor, 1964). The average Cr value in Salwa Bay was generally below those listed in Table 4, with the exception of the Aqeer coastline in the Arabian Gulf (Al-Hashim et al., 2021). Furthermore, the average As value in Salwa Bay was lower than reported in Table 4, except for the Red Sea-Gulf of Aqaba coastline (El-Sorogy et al., 2020) and Al-Khobar, Saudi Arabia (Alharbi and El-Sorogy, 2017).

3.2. Ecological risk assessment and potential sources of heavy metal(loid)s

Table 4 illustrates the class distribution (sample %) of enrichment factor (EF), geo-accumulation index (Igeo), and contamination factor (CF) for the heavy metal(loid)s analyzed in the sediment samples of the study area. The Igeo and CF values for the HMs reveal that all sediment samples fall into class 0 and class 1, respectively, indicating uncontaminated and low contamination levels (Weissmannová and Pavlovský, 2017). The EF class distribution results indicate that 6.66 % of the sediment samples exhibit very high enrichment with As. Additionally, 66.67 %, 26.67 %, and 3.33 % of the samples show significant enrichment with As, Pb, and Cu, respectively. However, moderate enrichment is observed in 26.67 % of the samples for As, 30 % for Cr and Zn, 16.67 % for Cu, 40 % for Ni, and 60 % for Pb (refer to Table 4).

Table 5
Minimum, maximum and average values of EF, Igeo, and CF in Salwa coastal sediment.

HMs	Indices	Minimum	Maximum	Average
Pb	EF	1.12	16.52	4.81
	Igeo	−2.71	−1.61	−2.25
	CF	0.05	0.15	0.08
Zn	EF	1.24	4.97	2.18
	Igeo	−3.57	−1.78	−2.85
	CF	0.02	0.13	0.05
Cr	EF	1.31	4.12	2.09
	Igeo	−4.21	−1.12	−2.86
	CF	0.01	0.24	0.06
Ni	EF	0.58	3.08	1.95
	Igeo	−4.62	−1.04	−2.93
	CF	0.01	0.26	0.07
Cu	EF	0.70	5.24	1.69
	Igeo	−6.59	−4.08	−5.65
	CF	0.02	0.09	0.03
As	EF	2.59	29.05	9.30
	Igeo	−4.29	−1.48	−3.23
	CF	0.08	0.54	0.18

EF values play a crucial role in distinguishing between elements influenced by human activities and those of geological origin (Reimann and de Caritat, 2005; Kahal et al., 2020). The average values of EF for the HMs in a descending order are recognized as As (9.30) > Pb (4.81) > Zn (2.18) > Cr (2.09) > Ni (1.95) > Cu (1.69). This indicates that the coastal sediments of Salwa Bay exhibit a significant enrichment in As, moderate enrichment in Pb, Zn, Cr, and deficiency to minimal

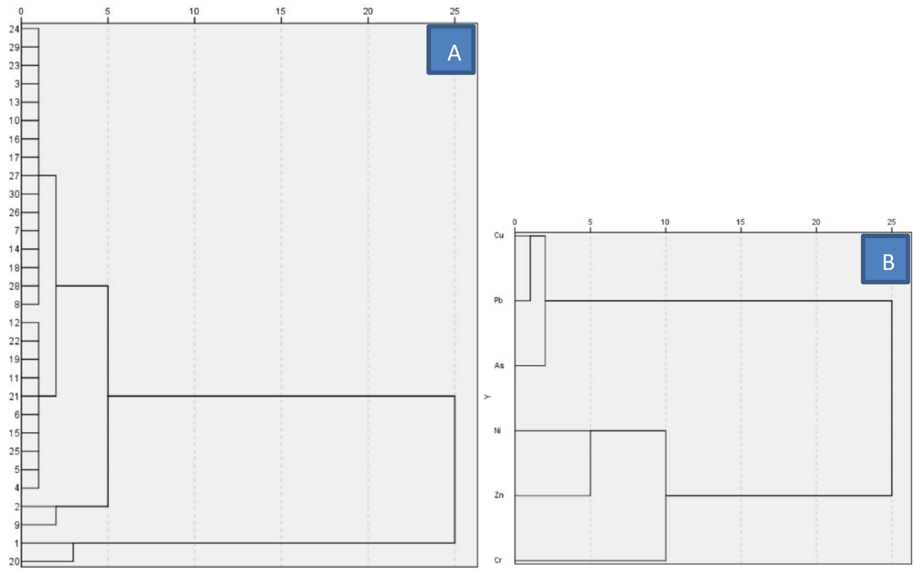

Fig. 3. A. Q mode-HCA of soil samples; B. R mode-HCA of HMs.

Table 6
The correlation matrix of the analyzed HMs.

	As	Cr	Cu	Ni	Pb	Zn
As	1					
Cr	0.393*	1				
Cu	0.421*	**0.849****	1			
Ni	0.493**	**0.928****	**0.807****	1		
Pb	0.085	**0.616****	**0.602****	**0.553****	1	
Zn	**0.541****	**0.890****	**0.760****	**0.962****	**0.543****	1

*. Correlation is significant at the 0.05 level (2-tailed).
**. Correlation is significant at the 0.01 level (2-tailed).

Table 7
Principal component for the investigated HMs.

	Component	
	PC1	PC2
As	**0.546**	**0.533**
Cr	**0.945**	−0.125
Cu	**0.835**	−0.295
Ni	**0.977**	−0.008
Pb	**0.614**	−0.616
Zn	**0.975**	0.077
% of Variance	65.66	14.55
Cumulative %	65.66	80.22

enrichment for Ni, and Cu. For As, S27 and S30 showed EF values exceeded 20, implying very high enrichment with this metal(loid). Moreover, S7, S14, S18, and S26-S30 showed significant enrichment in Pb. The average values of the contamination indices (Table 5) indicate that the HMs in sediments of the Salwa Bay are predominantly of natural geological origin rather than being significantly influenced by human activities (Alzahrani et al., 2023b). In comparison with the range of ERL and ERM values for sediment quality guidelines (SQG) of Long et al. (1995) in Table 4, it is noticed that all reported values of Cu, Ni, Zn, As, Cr, and Pb were below the ERL, indicating that the coastal sediments under study do not pose a risk to benthic communities due to the presence of HMs (Valdés and Tapia, 2019).

The Q-mode hierarchical cluster analysis (HCA) classified the 30 samples into three clusters (Fig. 3A). Cluster 1 consists of samples S1 and S20, which exhibit the highest concentrations of Cr, Cu, Pb, Ni, and Zn. The second cluster comprises samples S3-S8, S10-S19, and S21-S30, exhibiting the most minimal levels of all the assessed heavy metals. The third cluster consists of samples S2 and S9, which display the highest concentration of arsenic (As) and elevated levels of heavy metals (HMs) compared to the first and second clusters. The samples S1, S2, S9, and S20 were found in the southern region of Salwa Bay, in separate locations away from the open sea. These samples were composed of sediments with a fine to very fine particle size. As a result, they showed elevated concentrations of metal(loid)s, as reported by Vieira et al. (2021) and Alarifi et al. (2023). R-mode Hierarchical clustering analysis (HCA) categorized the HMs into two distinct clusters (Fig. 3B). The initial cluster comprises the elements As, Pb, and Cu, whereas the subsequent cluster encompasses Ni, Zn, and Cr. The average levels of arsenic (As), lead (Pb), and copper (Cu) showed high, moderate, and low enrichment of these HMs, respectively, indicating that they likely originated from human activities. On the other hand, the contamination indices suggested that the HMs of the second cluster originated from natural sources in the Earth's crust (Kahal et al., 2018). However, the average value of Zn indicated moderate enrichment, implying some anthropogenic factors.

Pearson's correlation analysis in Table 6 reveals a strongly positive correlation between Zn and each of As, Cr, Cu, Ni, and Pb (r = 0.541, 0.890, 0.760, 0.962, and 0.543, respectively). This suggests similar sources for these elemental pairs (El-Sorogy et al., 2016b; Nour et al., 2022). On the other hand, weak correlations were observed between As and the remaining HMs, except for Zn, indicating different sources for these two elements, likely of anthropogenic origin. These findings are further supported by principal component analysis (PCA), which identified two principal components (PCs) explaining 65.66 % and 14.55 % of the total variance, respectively (Table 7). PC1 exhibited high loading for As, Cr, Cu, Ni, Pb, and Zn, while PC2 showed high loading for As. The presence of As in both PCs implies a mixture of anthropogenic and natural sources for this metalloid. Nevertheless, on-site examinations revealed that the act of depositing waste in landfills as a result of coastal development, the presence of desalination plants, oil spills, and petrochemical industries were the human-caused pollutants in the Arabian Gulf and Salwa Bay (Alzahrani et al., 2023a; El-Sorogy et al., 2024).

3.3. Health risk assessment

Heavy metal(loids) exist in sediments and soils in various forms including free ions, soluble inorganic and organic complexes, carbonate-bound, iron and manganese oxide-bound, solid-state organic matter-bound, or as residual metals, exhibiting differences in mobility,

Table 8
Average CDI values (mg/kg/day) for non-carcinogenic possibility in adults and children.

Metal(loid)s		Ingestion	Dermal
As	Adult	3.05251E-06	1.22E-08
	Children	2.84901E-05	5.68E-08
Cr	Adult	7.07763E-06	2.82E-08
	Children	6.60578E-05	1.32E-07
Pb	Adult	2.23744E-06	8.93E-09
	Children	2.08828E-05	4.17E-08
Cu	Adults	1.99543E-06	7.96E-09
	Children	1.8624E-05	3.72E-08
Ni	Adults	1.76256E-05	7.03E-08
	Children	0.000164505	3.28E-07
Zn	Adults	6.11872E-06	2.44E-08
	Children	5.71081E-05	1.14E-07

bioavailability, and chemical reactivity (Oves et al., 2012; Alloway, 2013). These HMs pose a significant risk to both ecosystems and human health due to their high toxicity (Heidari et al., 2021; Miletic et al., 2023). Because of the detrimental effects they can have on humans, plants, and animals, HMs such as As, Cr, and Pb garner considerable public attention (Zhang et al., 2022).

The average chronic daily intake (CDI) values in mg/kg/day for possibility of non-carcinogenic effects in adults exhibited a range from 7.07763E-06 (Cr) to 1.76256E-05 (Ni) for the ingestion pathway and from 7.96E-09 (Cu) to 7.03E-08 (Ni) for the dermal pathway (Table 8). On the other hand, the CDI (mg/kg/day) for children ranged from 1.8624E-05 (Cu) to 0.000164505 (Ni) for the ingestion pathway and from 3.72E-08 (Cu) to 3.28E-07 (Ni) for the dermal pathway. These findings suggest a higher risk of non-carcinogenic exposure for children in both ingestion and dermal pathways as compared to adults.

The hazard index (HI) values for adults exhibited the following ranges: 0.0000060–0.0021 (Ni), 0.0000092–0.000055 (Zn), 0.000026–0.00015 (Cu), 0.00039–0.0012 (Pb), 0.00048–0.010 (As), and 0.0014–0.0091 (Cr). For children, the HI values ranged from 0.000085 to 0.00051 (Zn), 0.00024–0.0014 (Cu), 0.0032–0.020 (Ni), 0.0037–0.01099 (Pb), 0.0043–0.094 (As), and 0.013–0.085 (Cr) (Table S. 2). These results indicate that the cumulative hazard index was higher among children compared to adults (Fig. 4). However, it's noteworthy that all HI values for the metal(loid)s were less than 1.0, suggesting that there is no possibility of non-carcinogenic effects exposure for individuals residing along the coastline of Salwa Bay (Tian et al., 2020).

Accumulation of high levels of Cr, Pb, and As in the human body can lead to severe complications, including lung and stomach cancer, dermal lesions, respiratory system issues, and potential impacts on the nervous system, potentially causing renal failure (IARC, 1994; Mao et al., 2019). The excess lifetime cancer risk (ELCR) for adults showed a range from 6.877E-07 to 1.513E-05 for Cr, 1.169E-08 to 3.507E-08 for Pb, and 2.063E-06 to 1.444E-05 for As. In the case of children, ELCR varied from 6.405E-06 to 1.409E-04 for Cr, 1.089E-07 to 3.267E-07 for Pb, and 1.922E-05 to 1.345E-04 for As (Table S. 3). The spatial distribution of ELCR for As, Cr, and Pb across sample locations exhibited similar patterns for both children and adults, with higher values in children (Fig. 5). For adults, all ELCR values were below 1×10^{-4}, indicating no significant carcinogenic health risk for individuals residing along the coastline of Salwa Bay due to the presence of these HMs in sediments (Mondal et al., 2021). However, concerning children, ELCR values were below 1×10^{-6} for Pb, suggesting no substantial health hazards. Yet, ELCR values exceeded the threshold of 1×10^{-4} in sampling sites S1 and S20 for Cr and in S9 for As, indicating a potential lifetime carcinogenic risk for children in these specific locations (Zhao et al., 2014; Pan et al., 2018).

4. Conclusions

This study sheds light on the contamination of heavy metal(loid)s and the associated human health risks along the shores of Salwa Bay, Saudi Arabia. The average concentrations of metal(loid)s followed the order: Cr > Zn > Ni > As > Pb > Cu. Notably, the southern part of Salwa Bay exhibited higher levels of metal(loid)s compared to its northern counterpart. Average EF values indicated a significant enrichment in As, moderate enrichment in Pb, Zn, Cr, and deficiency to minimal enrichment for Ni, and Cu. Despite the observed contamination, the average HI values were less than 1.0, suggesting negligible possibility of non-carcinogenic effects for individuals inhabiting the coastline of Salwa Bay. Additionally, the ELCR values for adults were less than 1×10^{-4}, indicating no significant carcinogenic health risks associated with the presence of Pb, Cr, and As in the sediments. However, for children, ELCR values were less than 1×10^{-6} for Pb, indicating no risk. Mitigation measures should be taken in accordance with the standards within the bay to prevent increasing the potential risks of pollution.

Authorship contributions

[KA], [ASE] and [MHA] collecting samples, preparing samples for chemical analysis, writing manuscript and interpreting chemical analysis. [ASE] submitting the manuscript. All authors read and approved

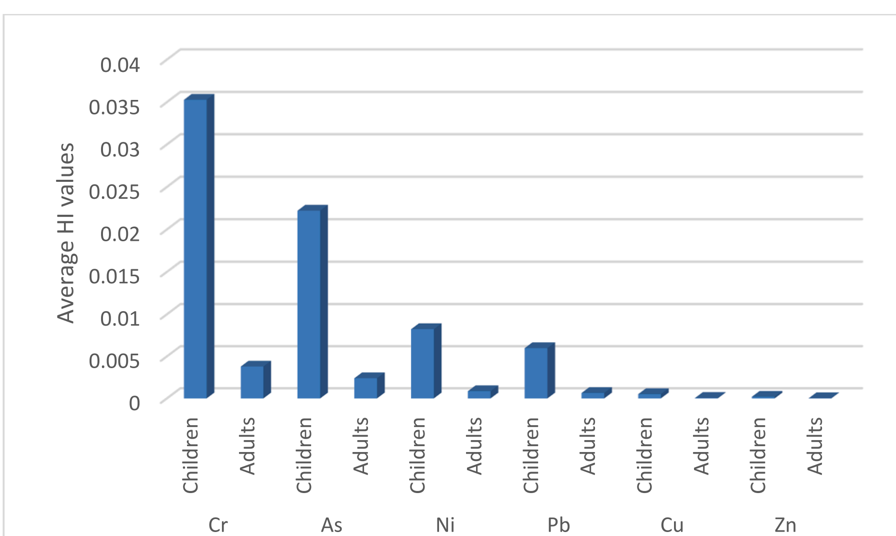

Fig. 4. The average HI values for possibility of non-carcinogenic effects in adults and children.

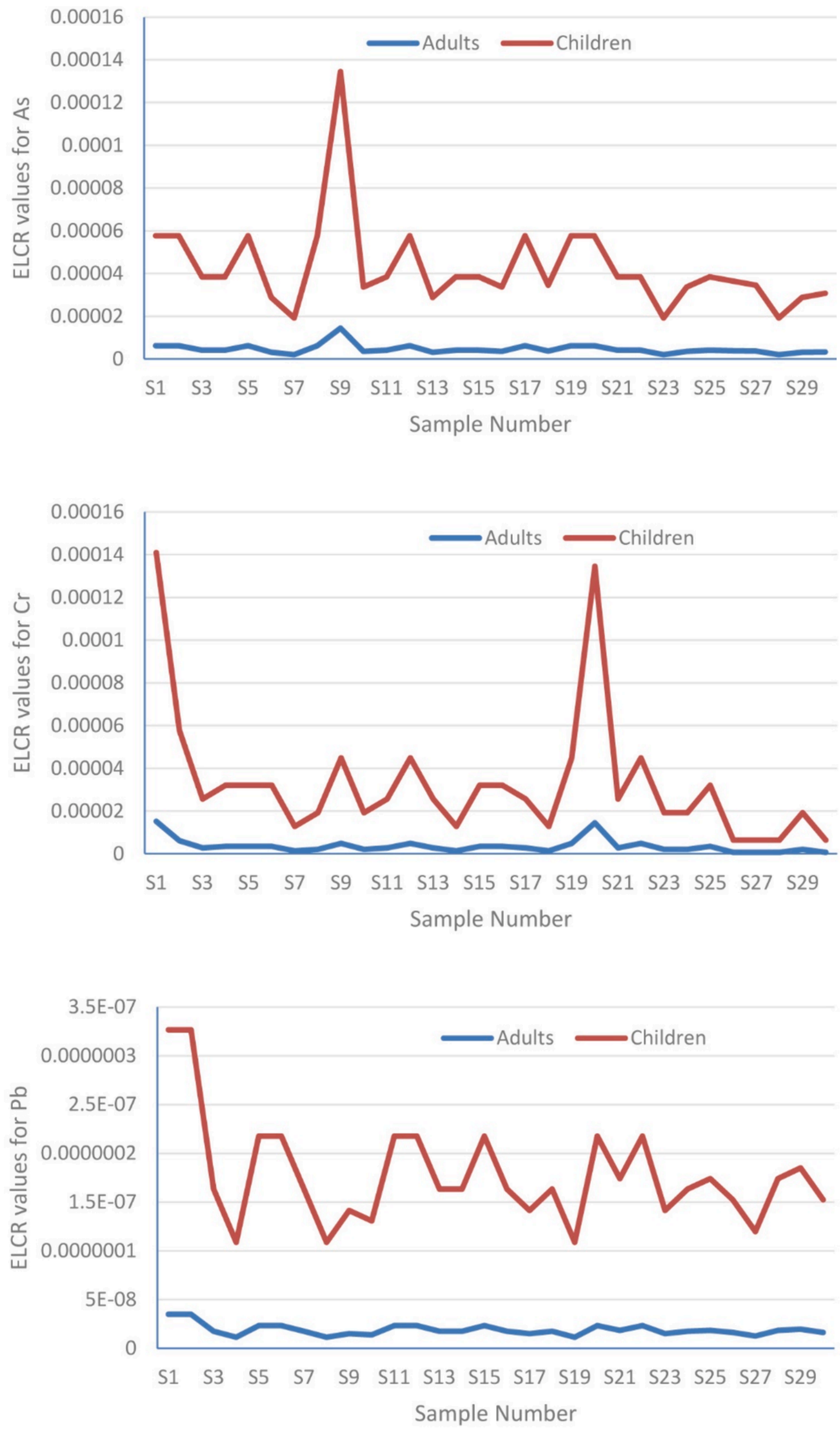

Fig. 5. Distribution of ELCR values for As, Cr, and Pb in children and adults per sampled locations.

the final manuscript.

CRediT authorship contribution statement

Khaled Al-Kahtany: Conceptualization, Funding acquisition, Methodology, Project administration, Supervision, Writing – original draft, Writing – review & editing. **Mansour H. Al-Hashim:** Investigation, Methodology, Software, Writing – original draft, Writing – review & editing. **Abdelbaset S. El-Sorogy:** Methodology, Writing – original draft, Writing – review & editing.

Declaration of competing interest

The authors declare that they have no known competing financial interests or personal relationships that could have appeared to influence the work reported in this paper.

Acknowledgments

The authors extend their appreciation to Researchers Supporting Project number (RSP2024R139), King Saud University, Riyadh, Saudi Arabia.

Appendix A. Supplementary data

Supplementary data to this article can be found online at https://doi.org/10.1016/j.arabjc.2024.105868.

References

Abbaspour, N., Hurrell, R., Kelishadi, R., 2014. Review on iron and its importance for human health. J. Res. Med. Sci. 19 (2), 164–174.
Alarifi, S.S., El-Sorogy, A.S., Al-kahtany, Kh., Hazaea, S.A., 2023. Contamination and health risk assessment of potentially toxic elements in Al-Ammariah agricultural soil, Saudi Arabia. J. King Saud Univ. – Sci. 35, 102826.
Alharbi, T., Alfaifi, H., Almadani, S.A., El-Sorogy, A., 2017. Spatial distribution and metal contamination in the coastal sediments of Al-Khafji area, Arabian Gulf, Saudi Arabia. Environ. Monit. Assess. 189, 634.
Alharbi, T., El-Sorogy, A., 2017. Assessment of metal contamination in coastal sediments of Al-Khobar area, Arabian Gulf, Saudi Arabia. J. Afr. Earth Sc. 129, 458–468.
Alharbi, T., El-Sorogy, A.S., 2023. Risk assessment of potentially toxic elements in agricultural soils of Al-Ahsa Oasis, Saudi Arabia. Sustainability 15, 659. https://doi.org/10.3390/su15010659.
Alharbi, T., Nour, H., Al-Kahtany, Kh. Giacobbe, S., El-Sorogy, A. S., 2023. Sediment's quality and health risk assessment of heavy metals in the Al-Khafji area of the Arabian Gulf, Saudi Arabia. Environ. Earth Sci. 82:471. doi: 10.1007/s12665-023-11171-z.
Al-Hashim, M.H., El-Sorogy, A.S., Al Qaisi, S., Alharbi, T., 2021. Contamination and ecological risk of heavy metals in Al-Uqair coastal sediments, Saudi Arabia. Mar. Pollut. Bull. 171, 112748.
Al-Kahtany, K., El-Sorogy, A.S., 2022. Heavy metal contamination of surface seawaters in Abu Ali Island, Saudi Arabia. Arab. J. Geosci. 15, 1662.
Al-Kahtany, Kh., El-Sorogy, A.S., 2023. Contamination and health risk assessment of surface sediments along Ras Abu Ali Island, Saudi Arabia. J. King Saud Univ.– Sci. 35, 102509 https://doi.org/10.1016/j.jksus.2022.102509.
Alloway, B.J. (Ed.) Heavy Metals in Soils: Trace Metals and Metalloids in Soils and Their Bioavailability; Environmental Pollution; Springer: Dordrecht, The Netherlands, 2013; Volume 22, ISBN 978-94-007-4469-1.
Almahasheer, H., Al-Taisan, W., Mohamed, M.K., 2013. Mangrove deterioration in Tarut Bay on the Eastern Province of the Kingdom of Saudi Arabia. Pakhtunkhwa. J. Life Sci. 1, 49–59.
Almasoud, F.I., Usman, A.I., Al-Farraj, A.S., 2015. Heavy metals in the soils of the Arabian Gulf coast affected by industrial activities: analysis and assessment using enrichment factor and multivariate analysis. Arab J. Geosci. 8 (3), 1691–1703.
Alzahrani, H., El-Sorogy, A.S., Qaysi, S., 2023a. Assessment of human health risks of toxic elements in coastal area between Al-Khafji and Al-Jubail, Saudi Arabia. Mar. Pollut. Bull. 196, 115622 https://doi.org/10.1016/j.marpolbul.2023.115622.
Alzahrani, H., El-Sorogy, A.S., Qaysi, S., Alshehri, F., 2023b. Contamination and risk assessment of potentially toxic elements in coastal sediments of the area between Al-Jubail and Al-Khafji, Arabian Gulf, Saudi Arabia. Water 15, 573. https://doi.org/10.3390/w15030573.
Amao, A.O., Kaminski, M.A., Babalola, L., 2018. Benthic foraminifera in hypersaline salwa bay (saudi arabia): an insight into future climate change in the gulf region? J. Foraminiferal Res. 48 (1), 29–40.
Aydin, H., Tepe, Y., Ustaoglu, F., 2023. A holistic approach to the eco-geochemical risk assessment of trace elements in the estuarine sediments of the Southeastern Black Sea. Mar. Pollut. Bull. 189, 114732 https://doi.org/10.1016/j.marpolbul.2023.114732.
Basson, P.W., Burchard, J., Jr., Hardy, J.T., Price, A.R., 1977. Biotopes of the Western Arabian Gulf; Marine Life and Environments of Saudi Arabia: ARAMCO Dhahran, 284 p.
Chen, H., Wang, L., Hu, B., Xu, J., Liu, X., 2022. Potential driving forces and probabilistic health pisks of heavy metal accumulation in the soils from an E-Waste Area, Southeast China. Chemosphere 289, 133182.
Clarke, M.H., Keij, A., 1973. Organisms as producers of carbonate sediment and indicators of environment in the southern Persian Gulf, *in* Purser, B. H. (ed.), The Persian Gulf: Springer-Verlag, Berlin, p. 33–56.
de Mora, S., Fowler, S.W., Wyse, E., Azemard, S., 2004. Distribution of heavy metals in marine bivalves, fish and coastal sediments in the Gulf and Gulf of Oman. Mar. Pollut. Bull. 49, 410–424.
Demircan, H., El-Sorogy, A.S., Alharbi, T., 2021. Bioerosional structures from the Late Pleistocene coral reef, Red Sea coast, northwest Saudi Arabia. Turk. J. Earth Sci. 30, 22–37.
Demircan, H., El-Sorogy, A.S., Al-Hashim, M., Richiano, S., 2023. Taphonomic signatures on the pearl oyster Pinctada from Arabian Gulf, Saudi Arabia. J. King Saud Univ. – Sci. 35, 102870 https://doi.org/10.1016/j.jksus.2023.102870.
El-Sorogy, A.S., 2015. Taphonomic processes of some intertidal gastropod and bivalve shells from northern Red Sea coast, Egypt. Pakist. J. Zool. 47 (5), 1287–1296.
El-Sorogy, A.S., Alzahrani, H., 2024. Bioerosion and encrustation of the rocky shore dwellers along the Arabian Gulf, Northeast Saudi Arabia. J. King Saud Univ. – Sci. 36, 103062 https://doi.org/10.1016/j.jksus.2023.103062.
El-Sorogy, A.S., Attiah, A., 2015. Assessment of metal contamination in coastal sediments, seawaters and bivalves of the Mediterranean Sea coast, Egypt. Mar. Pollut. Bull. 101, 867–871.
El-Sorogy, A.S., Alharbi, T., Richiano, S., 2018. Bioerosion structures in high-salinity marine environments: A case study from the Al–Khafji coastline, Saudi Arabia. Estuarine Coast. Shelf Sci. 204, 264–272.
El-Sorogy, A.S., Demircan, H., Alharbi, T., 2020. *Gastrochaenolites* ichnofacies from intertidal seashells, Al-Khobar coastline, Saudi Arabia. J. Afr. Earth Sci. 171. http://www.ncbi.nlm.nih.gov/pubmed/103943.
El-Sorogy, A.S., Demircan, H., Al-Kahtany, Kh., 2021. Taphonomic signatures on modern molluscs and corals from Red Sea coast, southern Saudi Arabia. Palaeoworld. https://doi.org/10.1016/j.palwor.2021.07.001.
El-Sorogy, A.S., Al-Kahtany, Kh., Al-Hashim, M.H., Alharbi, T., 2024. Distribution and contamination of seashells in Salwa Bay, Saudi Arabia. J. Afric. Earth Sci. 211, 105186 https://doi.org/10.1016/j.jafrearsci.2024.105186.
El-Sorogy, A.S., Youssef, M., 2015. Assessment of heavy metal contamination in intertidal gastropod and bivalve shells from central Arabian Gulf coastline, Saudi Arabia. J. Afr. Earth Sci. 111, 41–53.
El-Sorogy, A., Youssef, M., Al-Kahtany, Kh., 2016b. Integrated assessment of the Tarut Island coast, Arabian Gulf, Saudi Arabia. Environ. Earth. Sci. 75, 1336.
El-Sorogy, A.S., Youssef, M., Al-Hashim, M.H., 2023. Water quality assessment and environmental impact of heavy metals in the red sea coastal seawater of Yanbu, Saudi Arabia. Water 15, 201. https://doi.org/10.3390/w15010201.
Hakanson, L., 1980. An ecological risk index for aquatic pollution control. A sedimentological approach. Water Res. 14, 975–1001.
Heidari, M., Darijani, T., Alipour, V., 2021. Heavy metal pollution of road dust in a city and its highly polluted suburb; quantitative source apportionment and source-specific ecological and health risk assessment. Chemosphere 273, 129656.
IARC., 1994. monographs on the evaluation of carcinogenic risks to humans. Some Ind. Chem. 60, 389–433.
IRIS, Program Database 2020. Available online: https://cfpub.epa.gov/ncea/iris/search/index.cfm (accessed on 18 September 2020).
Kahal, A., El-Sorogy, A.S., Qaysi, S., Almadani, S., Kassem, O.M., Al-Dossari, A., 2020. Contamination and ecological risk assessment of the Red Sea coastal sediments, southwest Saudi Arabia. Mar. Pollut. Bull. 154, 111125.
Kahal, A.Y., El-Sorogy, A.S., Qaysi, S.I., Al-Hashim, M.H., Al-Dossari, A., 2023. Environmental risk assessment and sources of potentially toxic elements in seawater of Jazan Coastal Area, Saudi Arabia. Water 15, 3174. https://doi.org/10.3390/w15183174.
Kodat, M., Tepe, Y., 2023. A holistic approach to the assessment of heavy metal levels and associated risks in the coastal sediment of Giresun, Southeast Black Sea. Heliyon 9 (6), e16424.
Kowalska, J.B., Mazurek, R., Gasiorek, M., Zaleski, T., 2018. Pollution indices as useful tools for the comprehensive evaluation of the degree of soil contamination–A review. Environ. Geochem. Health 40, 2395–2420.
Long, E., MacDonald, D., Smith, S., Calder, F., 1995. Incidence of adverse biological effects within ranges of chemical concentrations in marine and estuarine sediments. Environ. Manage. 19, 81–97.
Luo, X.S., Ding, J., Xu, B., Wang, Y.J., Li, H.B., Yu, S., 2012. Incorporating bioaccessibility into human health risk assessments of heavy metals in urban park soils. Sci. Total Environ. 424, 88–96.
Luo, J., Ye, Y., Gao, Z., Wang, W., 2014. Essential and nonessential elements in the red-crowned crane Grus japonensis of Zhalong Wetland, northeastern China. Toxicol. Environ. Chem. 96 (7), 1096–1105.
Ma, J., Pan, L.B., Wang, Q., Lin, C.Y., Duan, X.L., Hou, H., 2016. Estimation of the daily soil/dust (SD) ingestion rate of children from Gansu Province, China via hand-to-mouth contact using tracer elements. Environ. Geochem. Health. doi: 10.1007/s10653-016-9906-1.
Manousi, N., Zachariadis, G.A., 2020. Development and application of an ICP-AES method for the determination of nutrient and toxic elements in savory snack products after autoclave dissolution. Separations 7, 66.
Mao, C., Song, Y., Chen, L., Ji, J., Li, J., Yuan, X., Yang, Z., Ayoko, G.A., Frost, R.L., Theiss, F., 2019. Human health risks of heavy metals in paddy rice based on transfer characteristics of heavy metals from soil to rice. Catena 175, 339–348.
Mazumder, D.G., 2008. Chronic arsenic toxicity & human health. Indian J Med Res 128 (4), 436–447.
Miletic, A., Lucic, M., Onjia, A., 2023. Exposure factors in health risk assessment of heavy metal(loid)s in soil and sediment. Metals 2023 (13), 1266. https://doi.org/10.3390/met13071266.
Mohammadi, A., Mansour, S.N., Najafi, M.L., Toolabi, A., Abdolahnejad, A., Faraji, M., Miri, M., 2022. Probabilistic risk assessment of soil contamination related to agricultural and industrial activities. Environ. Res. 203, 111837 https://doi.org/10.1016/j.envres.2021.111837.
Mondal, P., Lofrano, G., Carotenuto, M., Guida, M., Trifuoggi, M., Libralato, G., Sarkar, S. K., 2021. Health risk and geochemical assessment of trace elements in surface sediment along the hooghly (Ganges) River Estuary (India). Water 13, 110. https://doi.org/10.3390/w13020110.

Naser, H.A., 2013. Assessment and management of heavy metal pollution in the marine environment of the Arabian Gulf: a review. Mar. Pollut. Bull. 72, 6–13.

Nour, H.N., Alshehri, F., Sahour, H., El-Sorogy, A.S., Tawfik, M., 2022. Assessment of heavy metal contamination and health risk in the coastal sediments of Suez Bay, Gulf of Suez, Egypt. J. Afric. Earth Sci. 195, 104663 https://doi.org/10.1016/j.jafrearsci.2022.104663.

Oves, M., Khan, M.S., Zaidi, A., Ahmad, E. Soil Contamination, Nutritive Value, and Human Health Risk Assessment of Heavy Metals: An Overview. In Toxicity of Heavy Metals to Legumes and Bioremediation; Zaidi, A., Wani, P.A., Khan, M.S., Eds.; Springer: Vienna, Austria, 2012; pp. 1–27, ISBN 978-3-7091-0729-4.

Pan, L., Wang, Y., Ma, J., Hu, Y., Su, B., Fang, G., Wang, L., Xiang, B., 2018. A review of heavy metal pollution levels and health risk assessment of urban soils in Chinese cities. Environ. Sci. Pollut. Res. 25, 1055–1069. https://doi.org/10.1007/s11356-017-0513-1.

Rahman, M.S., Kumar, P., Ullah, M., Jolly, Y.N., Akhter, S., Kabir, J., Begum, B.A., Salam, A., 2021. Elemental analysis in surface soil and dust of roadside academic institutions in Dhaka city, Bangladesh and their impact on human health. Environ. Chem. Ecotoxicol. 3, 197–208.

Reimann, C., de Caritat, P., 2005. Distinguishing between natural and anthropogenic sources for elements in the environment: Regional geochemical surveys versus enrichment factors. Sci. Total Environ. 337, 91–107.

Riera, R., Tuya, F., Sacramento, A., Ramos, E., Rodŕıguez, M., Monterroso, Ó., 2011. The effects of brine disposal on a subtidal meiofauna community: Estuarine, Coastal Shelf Sci, 93, 359–365.

Shah, M.T., Ara, J., Muhammad, S., Khan, S., Tariq, S., 2012. Health risk assessment via surface water and sub-surface water consumption in the mafic and ultramafic terrain, Mohmand agency, northern Pakistan. J. Geochem. Explor. 118, 60–67. https://doi.org/10.1016/j.gexplo.2012.04.008.

Singovszka, E., Balintova, M., Demcak, S., Pavlikova, P., 2017. Metal pollution indices of bottom sediment and surface water affected by acid mine drainage. Metals 7, 284.

Taylor, S.R., 1964. Abundance of chemical elements in the continental crust: a new table. Geoch. Cosmoch. Acta 28, 1273–1285. https://doi.org/10.1016/0016-7037(64)90129-2.

Turekian, K.K., Wedepohl, K.H., 1961. Distribution of the elements in some major units of the earth's crust. Geol. Soc. Amer. 72, 175–192. https://doi.org/10.1130/0016-7606(1961)72[175:DOTEIS]2.0.CO;2.

USEPA, 2002. Supplemental guidance for developing soil screening levels for superfund sites. U. S. Environmental Protection Agency, Office of Emergency and Remedial Response, Washington.

USEPA, United States Environmental Protection Agency 2023. Regional Screening Levels (RSLs)—User's Guide. Available online: https://www.epa.gov/risk/regional-screeninglevels-rsls-users-guide.

Vieira, H.C., Bordalo, M.D., Figueroa, A.G., Soares, A.M.V.M., Morgado, F., Abreu, S.N., Rendon-von Osten, J., 2021. Mercury distribution and enrichment in coastal sediments from different geographical areas in the North Atlantic Ocean. Mar. Pollut. Bull. 165, 112153.

Weissmannová, H.D., Pavlovský, J., 2017. Indices of soil contamination by heavy metals –methodology of calculation for pollution assessment (minireview). Environ. Monit. Assess. 189, 616. https://doi.org/10.1007/s10661-017-6340-5.

Zhang, L., Yang, Z., Peng, M., Cheng, X., 2022. Contamination Levels and the Ecological and Human Health Risks of Potentially Toxic Elements (PTEs) in Soil of Baoshan Area, Southwest China. Appl. Sci. 12, 1693.

Zhao, L., Xu, Y., Hou, H., Shangguan, Y., Li, F., 2014. Source identification and health risk assessment of metals in urban soils around the Tanggu chemical industrial district, Tianjin, China. Sci. the Total Environ. 468–469, 654–662.